Inorganic Chemistry

Article

pubs.acs.org/IC

Copper Complexes Relevant to the Catalytic Cycle of Copper Nitrite Reductase: Electrochemical Detection of NO(*g*) Evolution and Flipping of NO_2 Binding Mode upon $Cu^{II} \rightarrow Cu^{I}$ Reduction

Ram Chandra Maji,[†] Suman Kumar Barman,[‡] Suprakash Roy,[†] Sudip K. Chatterjee,[†] Faye L. Bowles,[§] Marilyn M. Olmstead,[§] and Apurba K. Patra*[,†]

[†]Department of Chemistry, National Institute of Technology−Durgapur, Mahatma Gandhi Avenue, Durgapur 713 209, India

[‡]Department of Chemistry, Indian Institute of Technology−Kanpur, Kanpur 208 016, India

[§]Department of Chemistry, University of California-Davis, Davis, California 95616, United States

Supporting Information

ABSTRACT: Copper complexes of the deprotonated tridentate ligand, *N*-2-methylthiophenyl-2′-pyridinecarboxamide (HL1), were synthesized and characterized as part of our investigation into the reduction of copper(II) *o*-nitrito complexes into the related copper nitric oxide complexes and subsequent evolution of NO(*g*) such as occurs in the enzyme copper nitrite reductase. Our studies afforded the complexes $[(L1)Cu^{II}Cl]_n$ (**1**), $[(L1)Cu^{II}(ONO)]$ (**2**), $[(L1)Cu^{II}(H_2O)](ClO_4)\cdot H_2O$ (**3·H₂O**), $[(L1)Cu^{II}(CH_3OH)](ClO_4)$ (**4**), $[(L1)Cu^{II}(CH_3CO_2)]\cdot H_2O$ (**5·H₂O**), and $[Co(Cp)_2][(L1)Cu^{I}(NO_2)(CH_3CN)]$ (**6**). X-ray crystal structure determinations revealed distorted square-pyramidal coordination geometry around Cu^{II} ion in **1**−**5**. Substitution of the H_2O of **3** by nitrite quantitatively forms **2**, featuring the κ^2-O,O binding mode of NO_2^- to Cu^{II}. Reduction of **2** generates two Cu^{I} species, one with κ^1-O and other with the κ^1-N bonded NO_2^- group. The Cu^{I} analogue of **2**, compound **6**, was synthesized. The FTIR spectrum of **6** reveals the presence of κ^1-N bonded NO_2^-. Constant potential electrolysis corresponding to $Cu^{II} \rightarrow Cu^{I}$ reduction of a CH_3CN solution of **2** followed by reaction with acids, CH_3CO_2H or $HClO_4$ generates **5** or **3**, and NO(*g*), identified electrochemically. The isolated Cu^{I} complex **6** independently evolves one equivalent of NO(*g*) upon reaction with acids. Production of NO(g) was confirmed by forming [Co(TPP)NO] in CH_2Cl_2 (λ_{max} in CH_2Cl_2: 414 and 536 nm, ν_{NO} = 1693 cm^{-1}).

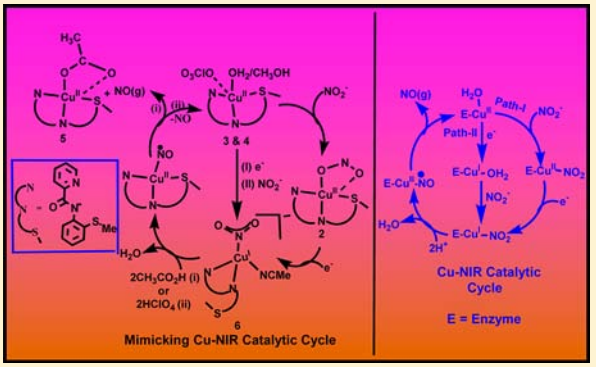

INTRODUCTION

Denitrification is an important biological process that involves the stepwise reduction of NO_3^- to N_2, as in $NO_3^- \rightarrow NO_2^- \rightarrow NO \rightarrow N_2O \rightarrow N_2$, which assists in the maintenance of an optimum level of nitrogen in the atmosphere.[1] The enzyme, copper nitrite reductase (CuNIR),[2] catalyzes the proton-coupled one-electron reduction of $NO_2^- \rightarrow NO$ ($NO_2^- + 2H^+ + e^- \rightarrow NO + H_2O$) and thus participates in the denitrification pathway. The resting-state enzyme has a Cu^{II} center bonded to three His-N and a H_2O molecule in a tetrahedral fashion, capable of binding NO_2^- by replacing H_2O.[2d] From X-ray structures and spectroscopic results, it is believed that the key reaction intermediate for CuNIR activity is a $Cu^{I}-NO_2$ species that may be envisioned to form via either the reduction of $Cu^{II}-NO_2$ (Scheme 1, Path-I) or reduction of the resting-state Cu^{II} aquo complex, followed by NO_2^- binding (Scheme 1, Path-II). In the oxidized Cu^{II} state, an asymmetric bidentate κ^2-O,O binding of nitrite occurs, and in the reduced Cu^{I} state, either κ^1-N (according to Averil et al.),[2a,b] or κ^2-O,O (according to Suzuki et al.),[2c] or κ^3-O,N,O (according to Hasnain et al.)[2d] binding mode of NO_2^- has been proposed, as shown in Scheme 1. One of the N−O bond cleavages of Cu^{I} bound NO_2^- in the presence of protons (Asp 98) generates an intermediate copper nitrosyl that eventually releases NO(*g*) and returns to the water bonded Cu^{II} resting state, thus sustaining the catalytic cycle.[2]

Several nitrite bound Cu^{II} (κ^1-O, κ^2-O,O, and κ^1-N bonded NO_2^-)[3,4] complexes and a few Cu^{I} (κ^1-O or κ^1-N bonded NO_2^-)[5] model complexes are reported, whereas the reactive and unstable copper nitrosyls are rarely isolated in the solid state. Only one example of a structurally characterized $Cu^{II}-NO^{\bullet}$, i.e., {Cu−NO}[10] species[6] and a few $Cu^{I}-NO^{\bullet}$, i.e., {Cu-NO}[11] species[7] are known. As the copper nitrosyls are reactive, in solution either the organic solvent[8] or the copper-coordinated ligand frame[9] is nitrosylated and the Cu^{I} species is depleted.

As a part of an investigation into whether the $Cu^{I}-NO_2$ complexes mimic functionally as CuNIR, it is necessary to explore their reactivity with acids in solution and to detect the

Received: May 27, 2013
Published: September 25, 2013

   dx.doi.org/10.1021/ic401295t | *Inorg. Chem.* 2013, 52, 11084−11095

Scheme 1. Proposed Mechanistic Pathway for Nitrite Reduction via Copper Nitrite Reductase (CuNIR)[a]

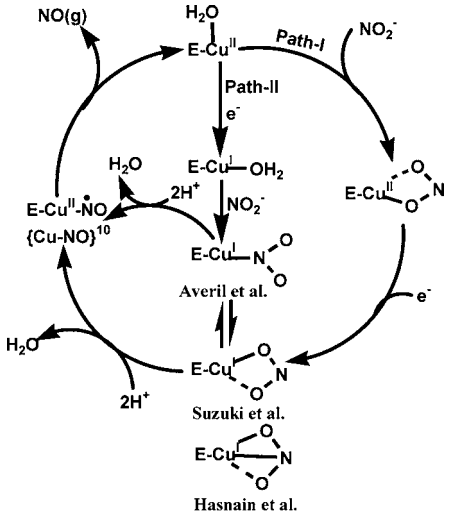

[a]E = enzyme.

generated intermediates such as copper nitrosyl (Cu-NO) or NO(g), using various spectroscopic techniques. For example, gas chromatography (GC) was used to detect and quantify evolved NO(g) from several model complexes.[4e,5a−g] A few examples are known where the liberated NO(g) has been allowed to react with (OEP)Fe,[5h] (EDTA)Fe,[3e] or (TPP)Co[5j] solution and then detected using ultraviolet-visible (UV-vis) spectroscopy of the respective stable metal nitrosyls. Lippard and co-workers and others have used fluorescence spectroscopy[10] for the chemical detection of NO. The use of NO-sensitive electrodes for the measurement of NO in biological systems is also known.[11] On the other hand, to detect the unstable Cu-NO adduct, Mondal and co-workers[9b−d] and others[4a,5i,7d] have used UV-vis and Fourier transform infrared (FTIR) spectroscopy. Herein, we report the synthesis, structure, electrochemical, and spectral properties of $Cu^{II/I}$ complexes of a tridentate carboxamide ligand, N-2-methylthiophenyl-2′-pyridinecarboxamide (HL1; see Scheme 2). The deprotonated

Scheme 2. Chemdraw Depiction of Ligand HL1 and Deprotonated Na^+L1^-

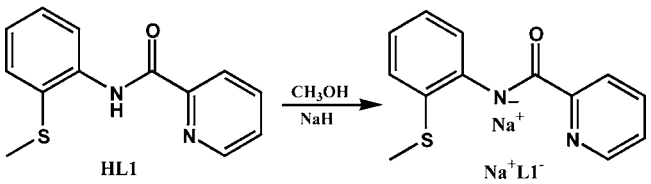

amidato N^- is a strong σ-donor ligand, expected to coordinate $Cu^{II/I}$ ion by proper tuning of its charge via delocalization and therefore, be amenable to production of $(L1)Cu^I-NO_2$ species and subsequent proton-coupled NO(g) evolution.

The synthesized and characterized $Cu^{II/I}$ complexes relevant to the catalytic cycle of CuNIR are shown in Scheme 3. Complexes **1**−**5** were structurally characterized to reveal $L1^-$ coordination via its amidato N^- donor. The H_2O or CH_3OH ligated complexes, **3** and **4**, readily react with NO_2^- to form **2**, where the NO_2^- is coordinated to Cu^{II} in an asymmetric κ^2-O,O fashion. Complex **2** in CH_3CN upon reduction converts to the corresponding Cu^I-NO_2 complexes such as $[(L1)Cu-ONO]^-$ and $[(L1)Cu(NO_2)]^-$, where κ^1-O and κ^1-N binding fashion of NO_2^- are involved, respectively, and confirmed electrochemically. Coulometrically reduced sample of **2**, or isolated Cu^I complex **6** itself in CH_3CN, reacts with CH_3CO_2H or $HClO_4$ that quantitatively generates NO(g) and the Cu^{II} complexes **5** or **3**, respectively, detected and quantified electrochemically. Simultaneous determination of NO(g) and the product metal complex (formed after NO liberation, e.g., **5** or **3**) using any of the above-mentioned three conventional methods (such as gas chromatography−thermal conductivity detection (GC-TCD), UV-vis of metal porphirinate nitrosyls, and NO-sensing electrode) has not been previously reported. In GC-TCD, the headspace NO(g) is used for sampling and its quantification.[4e,5a−g] Using a metal-porphyrin NO scavenger, diffusion of the generated headspace NO(g) from one vessel (where NO will generate) to the other (containing a solution of metal-porphyrin complex) is carried out.[5h,j] Both of these methods demand extra caution to account for the dissolved NO(g) left in the solvent that does not reach the headspace before its quantification. No such precaution is necessary for the electrochemical detection of NO(g) in solution, because it will dissolve immediately after its formation and will be readily available to the working electrode surface for its detection and quantification, up to a certain concentration.

EXPERIMENTAL SECTION

Materials and Reagents. Pyridine-2-carboxylic acid, 2-(methylthio)aniline, triphenylphosphite, sodium hydride, sodium perchlorate, $(n\text{-}Bu_4N)NO_2$, $Co(Cp)_2$, $(n\text{-}Bu_4N)ClO_4$, CD_3CN, pyrrole, benzaldehyde, propanoic acid were purchased from Aldrich Chemical Co. and used without further purification. CH_3CN, CH_3OH, C_2H_5OH, $CHCl_3$, CH_2Cl_2, C_5H_5N (pyridine), $(C_2H_5)_2O$ (diethyl ether), and n-hexane used either for spectroscopic studies or for syntheses were purified and dried following standard procedures prior to use. The ligand HL1 has been synthesized following a reported procedure.[12] $AgClO_4{\cdot}C_6H_6$ was prepared by recrystallization of $AgClO_4$ from hot benzene. Tetraphenyl porphyrin (TPP) was synthesized following a reported procedure (*J. Org. Chem.* **1967**, *32* (2), 476).

Synthesis Safety Note: *Transition-metal perchlorates are hazardous and explosive upon heating; therefore, these should be handled cautiously. No explosion occurred in the present study.*

Syntheses of Complexes. *$[(L1)CuCl]_n$ (1). Method A.* To a stirred solution of HL1 (0.3 g, 1.233 mmol) in 100 mL of CH_3OH was added solid NaH (29.6 mg, 1.233 mmol). The light yellow solution of NaL1 was added dropwise to a stirred solution of anhydrous $CuCl_2$ (165.8 mg, 1.233 mmol) in 30 mL of CH_3OH. The color changed to dark green. The solution was stirred for 8 h then allowed to slowly evaporate. After 4−5 days, dark green needle-shaped crystals of **1** were obtained, filtered off, washed with ether, and vacuum-dried (294 mg, 70%). Elemental analysis calcd for $C_{13}H_{11}N_2OSClCu$, **1**: C 45.61, H 3.24, N 8.18; Found: C 45.55, H 3.15, N 8.12; Selected IR frequencies (KBr disk, cm^{-1}): 3066(w), 3017(w), 2924(w), 1629(vs, $\nu_{C=O}$), 1598(vs), 1581(s), 1570(m), 1467(s), 1438(m), 1411(w), 1375(s), 1358(s), 1315(w), 1299(m), 1265(w), 1150(w), 1090(w), 1047(w), 1037(w), 1027(w), 977(w), 932(w), 911(w), 859(w), 809(w), 757(vs), 684(m), 652(w), 600(w), 516(w), 475(w), 437(w).

Method B. A CH_3OH solution (7 mL) of 35% HCl (19.2 mg, 0.184 mmol) was added dropwise to a stirred solution of **2** (synthesis of **2**: vide supra, 31 mg, 0.088 mmol) in 7 mL of CH_3OH. The resulting green solution was stirred for 4 h and kept for slow evaporation. After several days, green crystals of **1** were obtained, filtered off, washed with ether, and vacuum-dried (yield = 26 mg, 86%).

[(L1)Cu(ONO)] (2). Method A. To a stirred solution of **1** (200 mg, 0.584 mmol) in 35 mL of CH_3OH was added solid $NaNO_2$ (403 mg, 5.84 mmol). The resulting reaction mixture was stirred for 2 days and filtered. The filtrate was allowed to slowly evaporate and afforded

dx.doi.org/10.1021/ic401295t | *Inorg. Chem.* 2013, 52, 11084−11095

Scheme 3. Interconversion of Copper Complexes and Their Reactivities, Relevant to the Catalytic Cycle of CuNIR[a]

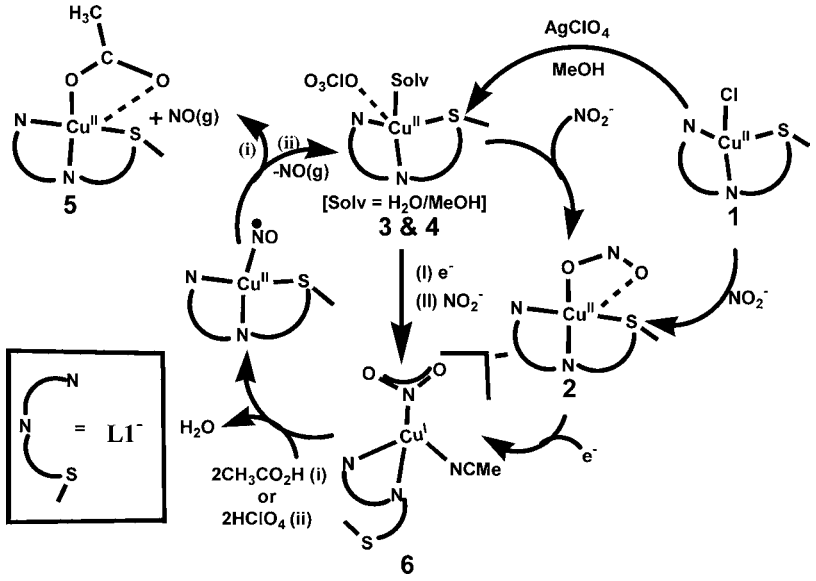

[a]Steps (i) and (ii) are when CH_3CO_2H and $HClO_4$ acids, respectively, are used as the proton source.

needle-shaped dark bluish green crystals of **2** after 5 days. The crystals were filtered off, washed with ether, and vacuum-dried (134.6 mg, 65%). Elemental analysis calcd for $C_{13}H_{11}N_3O_3S_1Cu_1$, **2**: C 44.25, H 3.14, N 11.91; Found: C 44.21, H 3.08, N 11.81; Selected IR frequencies (KBr disk, cm^{-1}): 3054(w), 3028(w), 2928(w), 1632(vs, $\nu_{C=O}$), 1601(vs), 1580(s),1570(m), 1467(vs), 1438(m), 1420(m), 1379(s), 1362(vs, $\nu(NO_2)$), 1298(m), 1266(m, $\nu(NO_2)$), 1244(w), 1150(w), 1116(m, $\nu(NO_2)$), 1048(w), 1038(w), 1028(w), 992(w), 970(w), 937(w), 903(w), 872(w), 832(w), 807(w), 767(vs), 752(vs), 723(w), 687(s), 653(m), 600(w), 516(w), 473(w), 437(w), 412(w).

Method B. To a stirred solution of HL1 (50 mg, 0.206 mmol) in 14 mL CH_3OH was added solid NaH (5.43 mg, 0.226 mmol). The yellow solution of NaL1 was added dropwise to a solution of $[Cu(CH_3CN)_4](ClO_4)_2$ (88 mg, 0.206 mmol) and $NaNO_2$ (21.3 mg, 0.309 mmol) in 6 mL CH_3OH. The resulting bluish green solution was stirred for 4 h and then kept for slow evaporation. After a few days, the bluish green crystals of **2** were obtained, filtered off, washed with ether, and vacuum-dried (yield = 52.4 mg, 72%).

Method C. To a stirred CH_3CN solution (6 mL) of **3** (50 mg, 0.113 mmol) or **4** (50 mg, 0.114 mmol) was added a CH_3CN solution (5 mL) of $(n\text{-}Bu_4N)NO_2$ (33 mg, 0.114 mmol). The resulting green solution was stirred for 2 h and kept for slow evaporation. After 4 days, green crystals formed that were filtered off, washed with water and ether, then vacuum-dried (yield = 36 mg, 90%).

*[(L1)Cu(H_2O)](ClO_4)·H_2O (**3·H_2O**).* To a stirred solution of **1** (50 mg, 0.146 mmol) in 10 mL CH_3OH was added 2 mL of a CH_3OH solution of $AgClO_4.C_6H_6$ (36 mg, 0.127 mmol) dropwise. The resulting blue solution was stirred overnight. AgCl was filtered through a Celite pad and filtrate was evaporated to dryness using a rotary evaporator that afforded a blue solid that was washed with water, ether, and vacuum-dried. The dry blue solid was then redissolved in crude CH_3CN, and to this solution, ether diffusion at 4 °C yielded dark blue crystals suitable for X-ray diffraction (XRD). Crystals were filtered off and washed with ether and vacuum-dried (yield = 49 mg, 79%). Elemental analysis calcd for $C_{14}H_{15}N_2O_6S_1Cl_1Cu_1$, **3·$H_2O$**: C 38.36, H 3.45, N 6.39. Found: C 38.21, H 3.42, N 6.27. Selected IR frequencies (KBr disk, cm^{-1}): 3450(br, ν(O−H)), 3108(w), 3067(w), 2924(m), 2856(w), 1630 (vs, ν(C═O)), 1597(vs), 1581(m), 1570(w), 1467(vs), 1438(w), 1375(s), 1359(s), 1299(m), 1265(w), 1147(s), 1100(s), 1079(s), 1048(w), 980(w), 932(w), 810(w), 756(s), 684(m), 655(w), 636(m), 625(w), 519(w), 474(w).

*[(L1)Cu(CH_3OH)](ClO_4) (**4**).* To a stirred solution of **2** (50 mg, 0.142 mmol) in 9 mL CH_3OH was added dropwise a CH_3OH solution (15 mL) of 70% perchloric acid (40.5 mg, 0.283 mmol). The color changed from green to bluish green. The resulting solution was stirred for 2 h then kept for slow evaporation. After 4 days, bluish green crystals of **4** were obtained, filtered off, washed with ether, and vacuum-dried (yield = 52 mg, 83.7%). Elemental analysis for $C_{14}H_{15}N_2O_6S_1Cl_1Cu_1$ (**4**): Calcd: C 38.36, H 3.45, N 6.39; Found: C 38.32, H 3.39, N 6.33; Selected IR frequencies (KBr disk, cm^{-1}): 3306(s, ν(OH)), 3106(w), 3059(w), 2997(w), 1654(s, overtone band of ν(OH)), 1626 (s, ν(C═O)), 1597(vs), 1580(m), 1570(m), 1535(m), 1482(m), 1466(s), 1436(w), 1379(w), 1364(s), 1314(w), 1296(w), 1261(w), 1105(vs), 1076(s), 1025(w), 951(w), 933(w), 915(w), 866(w), 813(w), 757(s), 687(w), 677(w), 646(w), 623, 519(w), 452(w).

*[(L1)Cu(CH_3CO_2)].H_2O (**5·H_2O**). Method A.* To a stirred solution of HL1 (50 mg, 0.205 mmol) in 5 mL CH_3OH was added dropwise an aqueous solution (2 mL) of $Cu(OAc)_2{\cdot}H_2O$ (41 mg, 0.205 mmol). The resulting green solution was stirred for 1 h and, to this solution, 10 mL of ether was layered and kept at 4 °C overnight. A green solid precipitated out and was filtered off, washed with ether and vacuum-dried (68 mg, 86%). The crystals suitable for XRD studies were grown from slow evaporation of a CH_3OH solution of this green solid. Elemental analysis for $C_{13}H_{11}O_4N_3S_1Cu_1$ (**5·H_2O**): Calcd: C 46.93, H 4.20, N 7.30; Found: C 46.76, H 4.09, N 7.27; Selected IR frequencies (KBr disk, cm^{-1}): 3524(vs, ν(OH)), 3440(vs, ν(OH)), 3064(w), 3014(w), 2928(w), 1618(vs, ν(C═O) + ν_a(COO)), 1594(vs), 1579(vs), 1469(vs), 1438(vs), 1392(vs), 1364(vs), 1336(vs), 1298(vs, ν_s(COO)), 1269(w), 1242(w), 1150(m), 1088(m), 1047(m), 1032(m), 1019(m), 981(m), 953(w), 934(m), 904(w), 879(w), 813(w), 774(s), 760(vs), 722(w), 689, 653, 618(w), 601(w), 518(w), 474(w).

Method B. To a stirred solution of **2** (50 mg, 0.141 mmol) in 10 mL of CH_3OH was added dropwise a solution of CH_3CO_2H (51 mg, 0.846 mmol) in 15 mL of CH_3OH. The color changed from bluish green to green. Distilled water (0.5 mL) was added and stirred for 4 h. The volume of the resulting reaction mixture was reduced to ∼10 mL by rotary evaporation and kept for slow evaporation. After 7 days, needle-shaped blue crystals of **5·H_2O** were obtained, filtered, washed with ether, and vacuum-dried (yield = 42.5 mg, 79%).

*[Co(Cp)$_2$][(L1)Cu(NO_2)(CH_3CN)] (**6**).* The reaction was performed inside a glovebox under N_2 atmosphere using dry degassed (freeze−pump−thaw) solvents. To a stirred greenish blue solution of **2** (50 mg, 0.141 mmol) in 4 mL of CH_2Cl_2 was added dropwise 4 mL of CH_2Cl_2 solution of $Co(Cp)_2$ (29 mg, 0.155 mmol). The solution color changed to brownish yellow and was stirred for 30 min and then 20 mL hexane was layered on top of the reaction mixture. After 3 h, the

dx.doi.org/10.1021/ic401295t | Inorg. Chem. 2013, 52, 11084−11095

Table 1. Data Collection and Structure Refinement Parameters for Complexes 1−5

complex	1	2	3·H_2O	4	5·H_2O
formulas	$C_{13}H_{11}N_2OSClCu$	$C_{13}H_{11}N_3O_3SCu$	$C_{13}H_{15}N_2O_7SClCu$	$C_{14}H_{15}N_2O_6SClCu$	$C_{14}H_{16}N_2O_4SCu$
mol wt	342.29	352.85	442.32	438.33	383.90
cryst. system	orthorhombic	triclinic	orthorhombic	monoclinic	monoclinic
color	green	purple	blue	blue-green	brown
space group	$Pca2_1$	$P\bar{1}$	$Pbca$	$P2_1/n$	$P2_1/c$
a, Å	20.580(2)	7.070(4)	7.6549(7)	7.6173(4)	7.032(2)
b, Å	4.1325(4)	10.986(7)	19.104(2)	19.0453(11)	17.395(5)
c, Å	15.3910(15)	17.650(11)	22.017(7)	11.2557(7)	13.098(4)
α, deg	90.0	105.695(14)	90.0	90.0	90.0
β, deg	90.0	92.008(6)	90.0	97.839(5)	99.315(7)
γ, deg	90.0	93.611(4)	90.0	90.0	90.0
V, Å^3	1308.9(2)	1315.2(14)	3219.8(11)	1617.65(16)	1581.0(8)
Z	4	4	8	4	4
d_{calc}, g cm^{-3}	1.737	1.782	1.825	1.800	1.613
θ range, deg	1.98−27.98	2.5375−32.261	2.53−39.93	2.90−31.50	1.963−30.593
μ, mm^{-1}	2.022	1.832	2.141	1.680	1.534
$F(000)$	692	716	1800	892	788
reflections/parameters	11210/173	19569/381	51872/243	18900/232	25338/242
unique reflections	2448	6067	6184	5171	4638
R_1 $[I > 2\sigma(I)]^a$	0.0329	0.0343	0.0355	0.0274	0.0283
wR_2 $[I > 2\sigma]^b$	0.0603	0.0844	0.0841	0.0758	0.0635
goodness of fit, GOF	1.000	1.033	1.054	1.092	1.187
res. dens., eÅ^{-3}	0.255/−0.427	1.028/−0.600	0.633/−1.095	1.059/−1.107	0.419/−0.341

$^a R_1 = \sum||F_o| - |F_c||/\sum|F_o|$. $^b wR_2 = \{\sum [w(F_o^2 - F_c^2)^2]/\sum w[(F_o^2)^2]\}^{1/2}$.

microcrystalline solid precipitated out and was filtered, washed with hexane, and dried (55 mg, 72%). Selected IR frequencies (KBr disk, cm^{-1}): 3429 (vs, ν(OH)), 3100 (m), 3017 (w), 2923(w), 2130 (w, ν(CN)), 1620 (vs, ν(C═O)), 1594 (vs), 1577 (s), 1567 (s), 1465 (vs) 1437 (w), 1413 (s), 1365 (vs), 1269 (s), 1092 (br, vs), 1010 (s), 864 (m), 814 (m), 761 (m), 690 (m), 620 (w), 460 (s); Elemental analysis for $C_{25}H_{24}ON_3SCuCo$ (**6**): C 55.91, H 4.50, N 7.82; Found: C 54.87, H 4.79, N 7.54. ^{1}H NMR (500 MHz, CD_3CN): δ 5.64 (1H, s, Cp proton), 5.42 (6H, s, of which 3H for Cp and 3H for either py or phenyl ring), 3.42 (2H, dd of py ring), 3.27 (6H, d, Cp), 2.15 (3H, s, −SCH_3), 1.939 (s, 3H, CH_3CN), 1.09 (3H, t, py, or phenyl ring proton). ESI mass spectrum m/z (%) negative mode: 439.97 [{(L1)Cu(NO_2)$_2$(CH_3CN) + 1H}, 98], 393.97 [{(L1)Cu(NO_2)-(CH_3CN) + 1H}, 100], 377.92 [{(L1)Cu(NO)(CH_3CN) + 1H}, 30]; positive mode: 189.008 [Co(Cp)$_2$, 100].

Crude Product (n-Bu_4N)[(L1)Cu(NO_2)]. The reaction was performed inside a glovebox under N_2 atmosphere using dry degassed (freeze−pump−thaw) solvents. Solid NaH (6 mg, 0.25 mmol) was added pinchwise to a stirred solution of HL1 (50 mg, 0.205 mmol) in 8 mL CH_3CN. A light yellow solution was generated that was stirred for 5 min and then solid [Cu(CH_3CN)$_4$](ClO_4) (68 mg, 0.208 mmol) was added. A dark red color developed immediately. Then, solid (*n*-Bu_4N)NO_2 (60 mg, 0.208 mmol) was added to this solution. The red color changes to brownish black. It was then stirred for 5 min and the solvent was removed completely to isolate a brownish black solid. Longer reaction times generate Cu^{II} via disproportionation: $2Cu^I \rightarrow Cu^{II} + Cu^0$. Selected IR frequencies (KBr disk, cm^{-1}): 3056 (w), 2964 (s), 2935(m), 2876 (m), 2015 (w, ν_{CN} of CH_3CN), 1621 (ν_{CO}, s), 1596 (s), 1578 (m), 1567 (m), 1466 (vs), 1438 (m), 1360 (br, s), 1295 (w), 1262 (m), 1091 (ν_{Cl-O} of ClO_4 present as an impurity), 882 (m), 815 (br, m), 756 (s), 690 (m), 647 (w), 622 (s), 516 (w), 456 (w), 412 (w). ^{1}H NMR (500 MHz, CD_3CN): δ 5.42 (2H, s, py ring ortho + py or phenyl), 3.41 (4H, dd, i.e. py (2H) + phenyl (2H) of 4 and 5 positions ring protons), 3.25 (d, 2H, Bu), 3.05 (6H, m, -Bu), 2.16 (3H, s, -SMe), 1.57 (8H, d, −Bu), 1.33 (6H, m, −Bu), 1.08 (6H, m, phenyl + py + −Bu proton), 0.94 (10H, t, −Bu). ESI mass spectrum m/z (%) negative mode: 440.17 [{(L1)Cu(NO_2)$_2$(CH_3CN) + 1H}, 100]; positive mode: 242.27 [*n*-Bu_4N, 100].

Physical Measurements. The FTIR spectra of the ligand and the complexes were recorded on a Thermo Nicolet iS10 or Bruker Vector 22 spectrometer, using KBr pellets, in the range of 4000−400 cm^{-1}. The electronic spectra were recorded on an Agilent 8453 diode array spectrophotometer. Elemental analyses were carried out on a Perkin−Elmer 2400 series-II CHNS Analyzer. Electron paramagnetic resonance (EPR) spectra were obtained in CH_3CN using a Bruker-EMX-1444 EPR spectrometer at 77 K. Mass spectra were recorded on Waters-HAB213 spectrometer. Solution conductivity was measured using CHEMILINE conductivity meter CL220, ^{1}H NMR spectra were recorded on JEOL JNM LA 500. Redox potentials were measured using CHI 1120A potentiometer. For constant potential electrolysis experiments, a platinum mesh working electrode was used and the solute concentration was kept at ∼(1−2) × 10^{-3} M.

X-ray Crystallography. Crystals of **1**, **2**, **4**, and **5** were grown via the slow evaporation of CH_3OH solution of the corresponding complexes at room temperature. Diethyl ether diffusion at low temperature (4 °C) to the CH_3CN solution of **3** yielded X-ray-quality crystals. Single-crystal intensity measurements for **1** were collected at 120(2) K, while those for **2**−**5** were collected at 90(2) K with a Bruker Smart APEX II CCD area detector, using either Mo Kα radiation (λ = 0.71073 Å) with a graphite monochromator (for **1**, **3**, **4**, and **5**) or synchrotron radiation with a Si(111) monochromator (for **2**). The cell refinement, indexing and scaling of the dataset were carried out using SAINT and Apex2 program.[13] All structures were solved by direct methods with SHELXS, and refined by full-matrix least-squares based on F^2 with SHELXL.[14] Other calculations were performed using WinGX, Ver 1.80.05.[15] The crystal of **2** shows two molecules in the asymmetric unit. The perchlorate anions present in **3** and **4** are not disordered. The Cu ion and the phenyl ring C atoms with its S-Me group is 7.1% disordered in **5**. The positions of the C-bound H atoms were calculated assuming ideal geometry and refined using a riding model. Figures showing displacement parameteres were created using the program XP.[16] Crystal data for the complexes **1**−**5** are summarized in Table 1. Additional crystallographic data and refinement details are available in CIF format in the Supporting Information.

dx.doi.org/10.1021/ic401295t | *Inorg. Chem.* 2013, 52, 11084−11095

RESULTS AND DISCUSSION

1. Synthesis and Characterization. Ligand HL1 has been prepared, following reported procedures,[12] and characterized by ^{1}H NMR and FTIR spectra (ν_{N-H} at 3278 cm^{-1} and $\nu_{C=O}$ at 1682 cm^{-1}). A solution of NaH in CH_3OH was used to deprotonate the ligand. Abstraction of chloride from **1** with the use of $AgClO_4\cdot C_6H_6$ in CH_3OH, formed **3** and **4**. The absence of ν_{N-H} and the red-shifted $\nu_{C=O}$ of **1** (1629 cm^{-1}), **2** (1632 cm^{-1}), **3** (1629 cm^{-1}), **4** (1624 cm^{-1}), **5** (1618 cm^{-1}), and **6** (1620 cm^{-1}) confirms the amidato N$^-$ ligation to Cu ions. Nitrite ligation occurred by addition of an equivalent amount of (n-Bu_4N)NO_2 to yield **3** or **4**; also, the reaction of excess $NaNO_2$ to **1** in CH_3CN yielded **2** in high yield. From the X-ray structure of **2** (vide supra), there are two molecules in the asymmetric unit. In one molecule, the N−O distances of the bound nitrite are 1.276(3) Å and 1.232(3) Å and in other molecule these are 1.282(3) Å and 1.228(2) Å. Interestingly, **2** displays strong bands in its IR spectrum (Supporting Information) at 1362 cm^{-1} that correspond to $\nu_a(NO_2)$ and at 1266 cm^{-1} that correspond to $\nu_s(NO_2)$ due to the chelating nitro group (κ^2-O,O) in first molecule and the corresponding two bands for other molecule are observed at 1380 cm^{-1} ($\nu_{N=O}$) and 1116 cm^{-1} (ν_{N-O}).[17] Casella and co-workers[3e] reported similar IR spectral behavior of the Cu^{II}-bound nitrite group (κ^2-O,O and κ^1-O bonded). Complex **2** reacts with HCl or CH_3CO_2H in CH_3OH and forms, quantitatively, **1** and **5**, respectively. Complex **5** can also be prepared from the reaction of an aqueous solution of $Cu(CH_3CO_2)_2\cdot H_2O$ to the ligand solution in CH_3OH ($CH_3CO_2^-$ acts as deprotonating agent and as a ligand). Strong stretching vibrations at 3520 cm^{-1} and 3440 cm^{-1} (ν_{OH}), 1618 cm^{-1} (ν_a(COO)) and 1298 cm^{-1} (ν_s(COO)) have been observed in the IR spectrum of **5** due to the H_2O and Cu^{II} coordinated $CH_3CO_2^-$ ion.

According to the proposed mechanisms,[2a−d] the key reaction intermediate; Cu^I−NO_2^-, may be envisioned to form either via the reduction of the nitrite bound Cu^{II} or via the reduction of resting-state Cu^{II} followed by nitrite binding, mentioned as Path-I and Path-II, respectively, in Scheme 1. Therefore, we have attempted to synthesize the NO_2^- bound Cu^I analogue of **2** via two possible ways (syntheses done in side glovebox using dry degassed solvents): synthesis of LCu^I(NO_2) via NO_2^- binding to (L1)Cu^I and synthesis of LCu^I(NO_2) via reduction of LCu^{II}(NO_2) using $Co(Cp)_2$, i.e., complex **6**.

(a). Synthesis of LCu^I(NO_2) via NO_2^- Binding to (L1)Cu^I. Reaction of L1$^-$ with [Cu^I(CH_3CN)$_4$](ClO_4) followed by addition of (n-Bu_4N)NO_2 in solvents such as $(CH_3)_2CO$, CH_3CN, CH_3OH (separate syntheses) generates a yellow solution. Solvent removal under vacuum yielded brownish black solid that was subjected to various spectroscopic studies such as FTIR, mass, and ^{1}H NMR spectroscopies. The solid in its FTIR spectrum display the $\nu_{C=O}$ at 1621 cm^{-1}, red-shifted from that of **2** (1632 cm^{-1}) which is expected as relatively electron-rich Cu^I pushes the electron density to the carbonyl group. Intense stretch at 2964 cm^{-1} is due to ν_{C-H} of Bu_4N^+ and the stretches at 1466 cm^{-1} ($\nu_a(NO_2)$), 1360 cm^{-1} ($\nu_s(NO_2)$), 1267, 815 cm^{-1} (δ(ONO)) and 456 cm^{-1} ($\nu_{CuN(nitrite)}$) are due to the κ^1-N bound NO_2^- group[17] (see the Supporting Information). Similar IR stretches for the structurally characterized κ^1-N bound Cu^I−NO_2 and[15]N isotope labeled Cu$^{I-15}NO_2$ complexes have been reported recently by Fujii and co-workers[5h] where δ(ONO) and $\nu_{Cu-N(nitrite)}$ have been observed at around 800 cm^{-1} and 400 cm^{-1}, respectively. The mass spectrum (see the Supporting Information) taken in CH_3CN features the molecular ion peak at 440.1779 (ESI negative) and at 242.2786 (ESI positive), which respectively correspond to the anion and cation of a complex of probable formulas (n-Bu_4N)[Cu^I(L1)(NO_2)(HNO_2)(CH_3CN)]. ^{1}H NMR in CD_3CN (sample prepared under N_2) features sharp signals (see the Supporting Information) within δ = 0−10 ppm. All these spectroscopic data reveals the formation of Cu^I species with bound NO_2^- group. In solution, this Cu^I sample is not stable enough for crystallization. Longer reaction time even under N_2 develop green color Cu^{II} species with a red color scum on the side wall of the reaction vessel, which is possibly due to the disproportionation reaction ($2Cu^I \rightarrow Cu^{II} + Cu^0$). From the green solution, the solid isolated is EPR active that display a strong signal at g = 2.0922 (see the Supporting Information), confirming that it is Cu^{II}.

*(b). Synthesis of LCu^I(NO_2) via Reduction of LCu^{II}(NO_2) Using Co(Cp)$_2$ (i.e., Complex **6**).* The reaction of CH_2Cl_2 solution of **2** with a dilute CH_2Cl_2 solution of $Co(Cp)_2$, followed by precipitation using dry hexane, changes to brownish black solid. The solid display stretches at 3100 cm^{-1} (ν_{CH}), 2130 cm^{-1} (ν_{CN} of CH_3CN), 1620 cm^{-1} (ν_{CO}), 1413 cm^{-1} ($\nu_a(NO_2)$), 1365 cm^{-1} ($\nu_s(NO_2)$), 814 cm^{-1} (δ(ONO)), 620 cm^{-1}($\rho_w(NO_2)$) and 460 cm^{-1} ($\nu_{CuN(nitrite)}$) (see the Supporting Information) that corroborates the κ^1-N binding mode of NO_2^- to Cu^I. Mass spectrum (CH_3CN) features peaks at 439.97 [(L1)Cu(NO_2)(HNO_2)(CH_3CN), 98%], 393.97 [(L1)Cu(HNO_2)(CH_3CN)], 100%], and 377.92 [(L1)Cu(HNO)(CH_3CN), 30%] in ESI negative mode and at 189.008 correspond to [Co(Cp)$_2$]$^+$ in positive mode (see the Supporting Information). The ^{1}H NMR spectrum of the isolated solid in CD_3CN, given in the Supporting Information, display sharp signals within δ = 0−10 ppm. The fact that the aromatic ring protons are shifted to higher field than δ ∼7 ppm indicates the nonplanarity of pyridine and phenyl rings to each other. Thus, the aromatic ring current of one, with respect to the other, opposes the applied magnetic field and shifts the resonance to higher δ.[18] Appreciably higher field shift of phenyl ring protons (in the range 0.4−2.6 ppm and 1.4−3.3 ppm) are known in the literature.[18b] It is noteworthy that a 1:1 mixture of **2** and $Co(Cp)_2$ in CD_3CN also display exactly the same ^{1}H NMR like the isolated solid, which confirms the integrity of the samples in solution and isolated solid **6**.

Solution conductivity measurement in CH_3CN reveals that **1**, **2**, and **5** are nonelectrolytic (Λ ranges from 4 Ω mol^{-1} cm^{-1} to 10 Ω mol^{-1} cm^{-1}), whereas **3** and **4** behave as 1:1 electrolytes (Λ ranges from 120 Ω mol^{-1} cm^{-1} to 145 Ω mol^{-1} cm^{-1}).[19] Mass spectral results, microanalytical data, ^{1}H NMR, and other information mentioned above of **1**−**6** support their formulations as stated.

Structures of the Complexes, 1−5. Perspective full molecule views of **1**, **2**, **5** and the cationic views of **3** and **4** are shown in Figures 1−5, along with their atom labeling schemes. Distorted square pyramidal coordination geometry around Cu^{II} has been observed in all cases. In **1**, the Cl$^-$ anion of one molecule coordinates axially to the other Cu^{II} ion, thus making a polymeric chain compound in the solid state. Three donors of the amide ligand occupy three sites of the square plane of which the amidato N$^-$ donor is *trans* to the fourth site of the plane. Stronger coordination of the amidato N$^-$ to Cu^{II} is evident in all cases; therefore, the Cu^{II}−N_{amide} distances (in the range of 1.930−1.946 Å) in **1**−**5** are shorter than the Cu^{II}−N_{py} distances (in the range of 1.9747−1.992 Å) in the respective complexes.

dx.doi.org/10.1021/ic401295t | Inorg. Chem. 2013, 52, 11084−11095

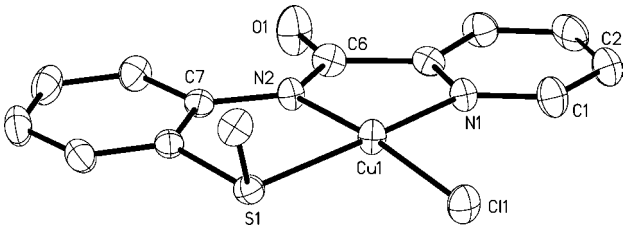

Figure 1. Thermal ellipsoid (probability level = 30%) plot of [(L1)CuCl] (**1**), along with the atom labeling scheme. H atoms are omitted for the sake of clarity.

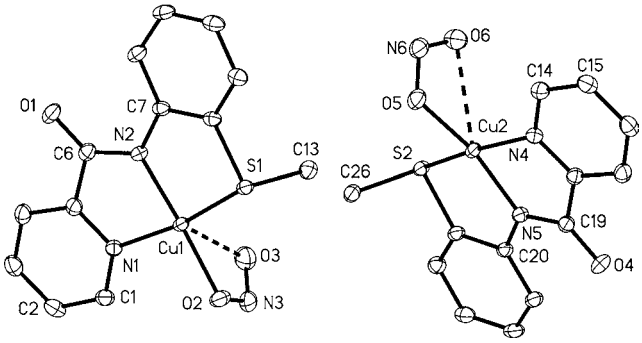

Figure 2. Thermal ellipsoid (probability level = 50%) plot of [(L1)Cu(ONO)] (**2**), along with the atom labeling scheme. H atoms are omitted for the sake of clarity. O3 and O6 occupy axial positions.

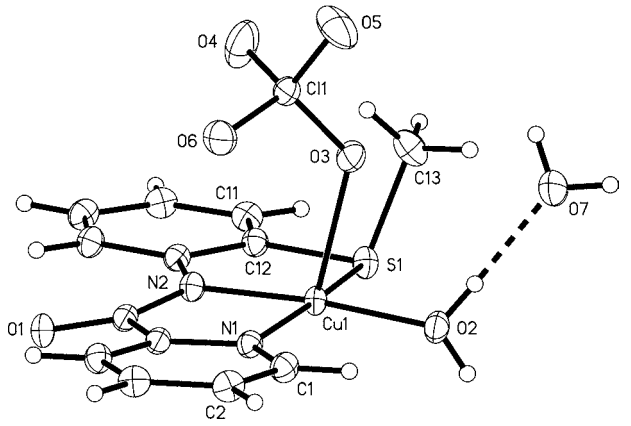

Figure 3. Thermal ellipsoid (probability level = 50%) plot of $[(L1)Cu(H_2O)](ClO_4)\cdot H_2O$ (**3·H₂O**), along with the atom labeling scheme.

The Cu^{II} ions are situated almost in the square plane, only 0.101, 0.099, 0.137, and 0.080 Å out of the plane toward the axial ligands in complexes **2**–**5**, respectively. The axial Cu^{II}–ligand bond is much longer than the other four, because of pseudo-Jahn–Teller distortion, which is commonly observed in Cu^{II} complexes.[20] Selected bond distances and angles of **1**–**5** are tabulated in Table 2.

In **2**, two molecules are present in the asymmetric unit. An average shorter Cu^{II}–O_{ONO} (in plane) and longer Cu^{II}–O_{ONO} (axial) distances of 1.9717(19) Å and 2.611(2) Å, respectively, strongly reveal the asymmetric κ^2-O,O binding fashion of the nitrite ion to Cu^{II} center(s) in both molecules (see Figure 2). Several reported structures of the oxidized state of CuNIRs reveal a typical asymmetric binding of the NO_2^- ion to Cu^{II} with a shorter Cu–O_{ONO} distance in the range 1.98–2.2 Å and

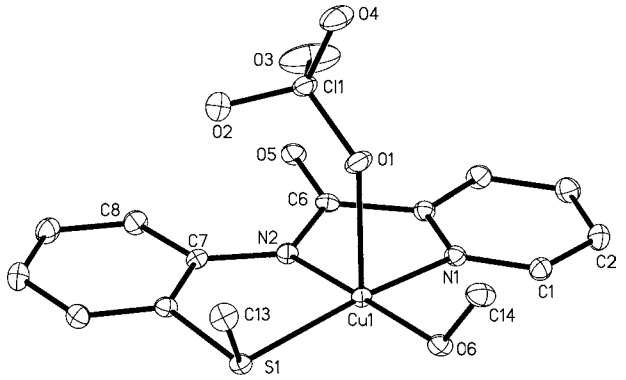

Figure 4. Thermal ellipsoid (probability level = 50%) plot of $[(L1)Cu(CH_3OH)](ClO_4)$ (**4**), along with the atom labeling scheme.

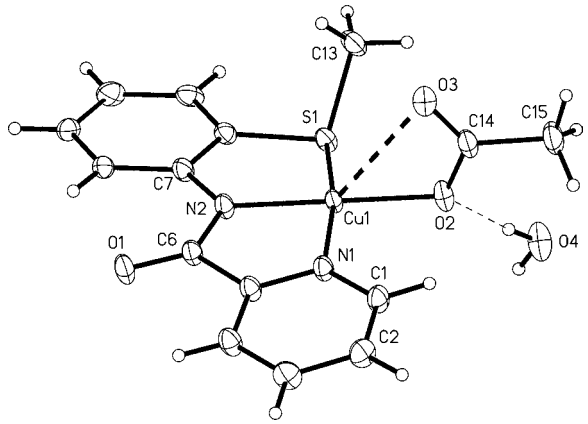

Figure 5. Thermal ellipsoid (probability level = 50%) plot of $[(L1)Cu(CH_3CO_2)]\cdot H_2O$ (**5·H₂O**), along with the atom labeling scheme.

the longer Cu–O_{ONO} in the range of 2.19–2.4 Å.[21] Model complexes with tripodal TEPA[3a] (where TEPA = triethyl-2-pyridylamine), various substituted Tp[3b–d] (where Tp = hydrotris(pyrazolyl)borate), 1-BB (bis[(1-methylbenzimidazol-2-yl)methyl]amine), and 2-BB (bis[2-(1-methylbenzimidazol-2-yl)ethyl]amine) ligands[3e–g] are known, where the longer Cu–O_{ONO} distance ranges from 2.031 Å to 2.678 Å. The angle ϕ between the O–N–O and O–Cu–O planes are very small (<1°) like other model complexes, which is in sharp contrast to that observed in native CuNIR that usually vary over the range of 60°–84° (the smallest known angle is 6°). The Cu–N_{ONO} distances of 2.678(3) Å (Cu1–N3) and 2.737(3) Å (Cu2–N6) in the two molecules of the asymmetric unit of **2** (Figure 2) are closer to the longer Cu–O_{ONO} distances of 2.554 Å (Cu1–O3) and 2.667 Å (Cu2–O6), respectively, than the shorter Cu–O_{ONO} distances of 1.9759 Å (Cu1–O2) and 1.9675 Å (Cu2–O5), respectively, similar to the trend observed in the oxidized CuNIR protein structures,[21] where these distances of Cu–N_{ONO} and longer Cu–O_{ONO} are found as 2.15 Å and 2.19 Å (for AcNIR), 2.31–2.36 Å and 2.29–2.38 Å (for AfNIR), 2.32 Å and 2.42 Å (for D98N AfNIR), and 3.21 Å and 3.60 Å (for H255N AfNIR), respectively. In **3** the water molecule present *trans* to the amidato N^- is strongly hydrogen-bonded to another water molecule present as a solvent of crystallization with an O2···O7 distance of 2.642(2) Å. In the case of the resting-state CuNIR, the Cu^{II}-bound water molecule is hydrogen-bonded to the O atom of the Asp(98) side chain (O of Cu^{II} coordinated H_2O to O of Asp-98 distance is 2.80

dx.doi.org/10.1021/ic401295t | *Inorg. Chem.* 2013, 52, 11084–11095

Table 2. Selected Bond Lengths (Å) and Angles (deg) for Complexes 1−5

[(L1)CuCl] (**1**)			
Bond Distances, Å			
Cu(1)−N(1)	1.984(3)	Cu(1)−S(1)	2.2881(9)
Cu(1)−N(2)	1.947(3)	Cu(1)−Cl(1)	2.2442(9)
Bond Angles, deg			
N(1)−Cu(1)−N(2)	83.36(11)	N(1)−Cu(1)−S(1)	167.84(8)
N(1)−Cu(1)−Cl(1)	97.14(8)	N(2)−Cu(1)−S(1)	85.96(8)
N(2)−Cu(1)−Cl(1)	172.12(9)	S(1)−Cu(1)−Cl(1)	92.65(4)
[(L1)Cu(ONO)] (**2**)			
Molecule 1		Molecule 2	
Bond Distances, Å			
Cu(1)−N(1)	1.992(2)	Cu(2)−N(4)	1.984(2)
Cu(1)−N(2)	1.930(2)	Cu(2)−N(5)	1.932(2)
Cu(1)−S(1)	2.3004(12)	Cu(2)−S(2)	2.2875(11)
Cu(1)−O(2)	1.9759(19)	Cu(2)−O(5)	1.9675(19)
Cu(1)−O(3)	2.554(2)	Cu(2)−O(6)	2.667(2)
Bond Angles, deg			
N(1)−Cu(1)−N(2)	83.62(9)	N(4)−Cu(2)−N(5)	83.46(9)
N(1)−Cu(1)−S(1)	168.27(6)	N(4)−Cu(2)−S(2)	165.59(6)
N(1)−Cu(1)−O(2)	95.21(8)	N(4)−Cu(2)−O(5)	95.61(8)
N(2)−Cu(1)−S(1)	87.05(7)	N(5)−Cu(2)−S(2)	87.25(7)
N(2)−Cu(1)−O(2)	176.09(7)	N(5)−Cu(2)−O(5)	164.86(8)
S(1)−Cu(1)−O(2)	93.63(7)	S(2)−Cu(2)−O(5)	96.21(7)
O(2)−N(3)−O(3)	115.1(2)	O(5)−N(6)−O(6)	115.1(2)
[(L1)Cu(H_2O)](ClO_4)3·H_2O			
Bond Distances, Å			
Cu(1)−N(1)	1.9798(13)	Cu(1)−S(1)	2.3126(5)
Cu(1)−N(2)	1.9367(12)	Cu(1)−O(2)	1.9551(11)
Cu(1)−O(3)	2.3907(12)	C(6)−O(1)	1.2459(16)
Bond Angles, deg			
N(1)−Cu(1)−N(2)	83.36(5)	S(1)−Cu(1)−O(2)	96.73(4)
N(1)−Cu(1)−S(1)	167.79(4)	O(3)−Cu(1)−N(1)	92.45(5)
N(1)−Cu(1)−O(2)	93.37(5)	O(3)−Cu(1)−O(2)	79.45(4)
N(2)−Cu(1)−S(1)	86.02(4)	O(3)−Cu(1)−N(2)	105.07(5)
N(2)−Cu(1)−O(2)	174.49(5)	O(3)−Cu(1)−S(1)	96.12(4)
[(L1)Cu(CH_3OH)](ClO_4) (**4**)			
Bond Distances, Å			
Cu(1)−N(1)	1.9747(15)	Cu(1)−S(1)	2.2991(5)
Cu(1)−N(2)	1.9395(15)	Cu(1)−O(1)	2.4264(14)
Cu(1)−O(6)	1.9627(13)	C(6)−O(5)	1.249(2)
Bond Angles, deg			
N(1)−Cu(1)−N(2)	83.69(6)	S(1)−Cu(1)−O(6)	94.55(4)
N(1)−Cu(1)−S(1)	164.60(5)	O(1)−Cu(1)−N(1)	92.33(6)
N(1)−Cu(1)−O(6)	94.35(6)	O(1)−Cu(1)−N(2)	93.43(6)
N(2)−Cu(1)−S(1)	86.80(5)	O(1)−Cu(1)−O(6)	89.26(5)
N(2)−Cu(1)−O(6)	176.74(6)	O(1)−Cu(1)−S(1)	100.32(4)
[(L1)Cu(CH_3CO_2)]5·H_2O			
Bond Distances, Å			
Cu(1)−N(1)	1.9875(13)	Cu(1)−S(1)	2.3101(7)
Cu(1)−N(2)	1.9319(13)	Cu(1)−O(2)	1.9391(12)
Cu(1)−O(3)	2.7766(13)	C(6)−O(1)	1.2367(17)
Bond Angles, deg			
N(1)−Cu(1)−N(2)	83.89(5)	S(1)−Cu(1)−O(2)	92.74(4)
N(1)−Cu(1)−S(1)	167.52(4)	O(3)−Cu(1)−N(1)	90.94(5)
N(1)−Cu(1)−O(2)	96.46(5)	O(3)−Cu(1)−O(2)	52.54(4)
N(2)−Cu(1)−S(1)	86.87(4)	O(3)−Cu(1)−N(2)	127.87(5)
N(2)−Cu(1)−O(2)	179.54(6)	O(3)−Cu(1)−S(1)	101.36(4)

Å).[2d] The trigonality index of τ = 0.071 for **1**, τ = 0.13 and 0.016 for two molecules of **2**, τ = 0.11 for **3**, and τ = 0.20 for **4** and **5** are comparable to those reported for square pyramidal Cu^{II} complexes of the N_2S donor ligand.[20]

Electronic Spectra. The electronic spectra of **1**−**5** were taken in CH_3OH, and the electronic spectra of **6** were taken in CH_3CN. The data are listed in Table 3. All complexes except **6**

Table 3. Electronic Absorption Spectral Data of 1−6 and HL1 Complexes at 298 K

	compound	λ_{max}, nm (ε, M^{-1} cm^{-1})
1	CH_3OH	258 (10400), 299 (5500), 310 (5590), 326 sh (5426), 455 sh (81), 642 (103)
2	CH_3OH	257 (14480), 298 (8540), 310 (8280), 327 sh (7730), 613 (157)
	CH_3CN	261 (15540), 301 sh (8263), 311 sh (7930), 330 sh (7080), 589 (133).
3	CH_3CN	260 (12740), 300 (8160), 312 sh (7630), 330 sh (6450) , 573 (190)
	H_2O	253 (15320), 295 sh (9640), 306 (9880), 322 sh (9200) , 451 sh (90), 625 (125)
	CH_3OH	258 (13000), 285 (7915), 297 (8050), 310 sh (7810), 330 sh (6940), 455 sh (110), 626 (150)
4	CH_3OH	259 (15855), 285 (10990), 296 sh (10540), 310 sh (9300), 328 (6900), 460 sh (87), 627 (110)
5	CH_3OH	259 (15420), 296 sh (8920), 310 sh (8500), 330 (7600) , 627(143)
6	CH_3CN	267 (25870), 335 (6300)
HL1	CH_2Cl_2	268 (5080), 287 (4000)

display a broad absorption band in the range of 613−642 nm, because of a d−d electronic transition (ε < 200 M^{-1} cm^{-1}). In the 300-nm region for **1**−**5**, three have been observed overlapped transitions (~300, ~310, and ~330 nm), and the spectral profiles for all these complexes are similar. Among these transitions, the relatively lower energy transition at ~330 nm is due to charge transfer from the monodentate ligand (*-trans* to amidato N) to Cu^{II} (see Figure 6). Other higher-energy transitions are due to the intraligand $n-\pi^*$ (300 and 310 nm) and $\pi-\pi^*$ transition (260 nm).

To check whether or not the water molecule ligated to Cu^{II} in **3** is easily replaceable by the externally added NO_2^- ion (required for the catalytic activity of CuNIR), we have titrated the CH_3CN solution of **3** with CH_3CN solution of (n-Bu_4N)(NO_2). The UV-vis traces obtained during titration are shown in Figure 7. The band position at 573 nm of **3** shifts to 579 nm, corresponding to the d−d band of **2**. The isosbestic points at 629, 478, 378, 332, and 291 nm clearly reveal the neat transformation of **3** → **2**. It is noteworthy, in the case of CuNIR, that the resting-state Cu^{II}-0bound water molecule provides the entry of NO_2^- ion in the catalytic cycle by replacing itself. To the best of our knowledge, at least one example of a $Cu^{II}-OH_2$ complex is reported in relation to the CuNIR modeling, where the bound water molecule has been shown to be replaced by NO_2^- ion in solution.[4c] To check the possibility of back replacement of NO_2^- by water, complex **2** was dissolved in CH_3OH/H_2O in the presence of $NaClO_4$ and slow evaporation yielded back **2**. The electronic spectrum of **6**

dx.doi.org/10.1021/ic401295t | *Inorg. Chem.* 2013, 52, 11084−11095

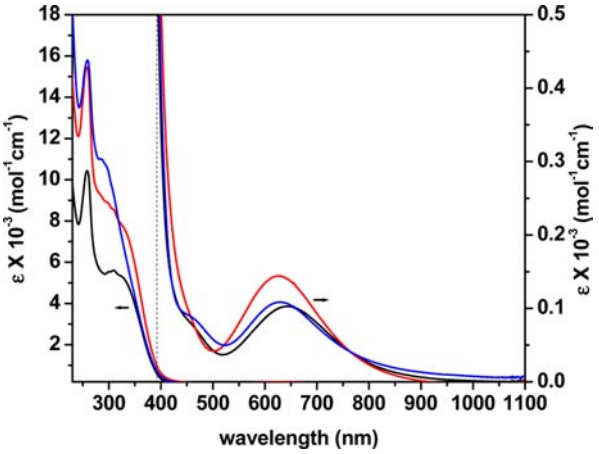

Figure 6. Electronic absorption spectra of **1** (black), **4** (blue), and **5** (red) in CH_3OH.

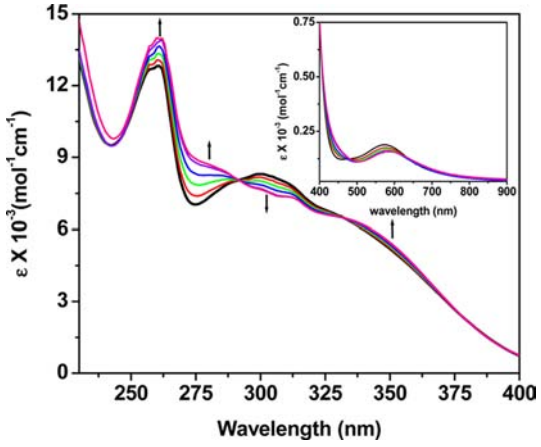

Figure 7. Electronic absorption spectral changes during transformation of **3** (black trace) → **2** (pink trace) when titrating a CH_3CN solution of **3** with a CH_3CN solution of $(n\text{-}Bu_4N)NO_2$.

taken in CH_3CN displays (see the Supporting Information) an intense shoulder at 335 nm, possibly due to the relatively electron-rich Cu^I to NO_2^- charge transfer, similar to the other reported Cu^I–NO_2 model complexes.[5]

Redox Properties and Nitrite Reductase Activity. For CuNIR activity, the easy access to the Cu^I–NO_2^- intermediate from its Cu^{II} precursor is necessary, which subsequently reduces the bound NO_2^- to NO. Therefore, the cyclic voltammograms of either Cu^{II}–NO_2^- or Cu^I–NO_2^- model complexes that highlight the accessibility of the $Cu^{II/I}$ oxidation states and their relative stability in solution in the designed ligand donor atoms environment are important. To investigate the susceptibility of the Cu^{II} center in complexes **1**–**5** toward oxidation or reduction, the cyclic voltammograms were recorded in CH_3CN using same cell setup. A three-electrode cell setup (such as platinum, saturated calomel electrode (SCE), and a platinum wire as the working, reference, and auxiliary electrodes, respectively) has been used to measure the potentials. Results are summarized in Table 4. The cyclic voltammograms of **1** in CH_3CN feature two irreversible reductions (see Figure 8): one at E_{pc} = −0.35 V and another

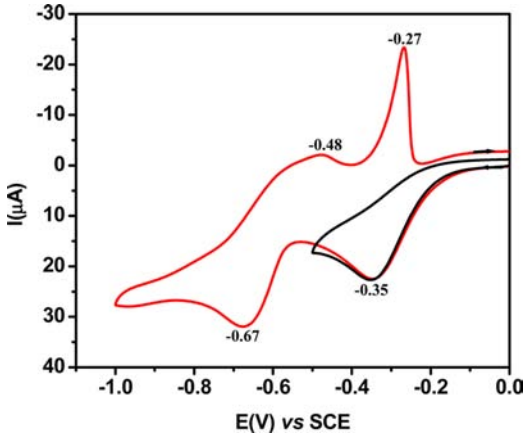

Figure 8. Cyclic voltammograms of **1** in CH_3CN containing 0.1 M [with $(n\text{-}Bu)_4N]ClO_4$ as a supporting electrolyte at 298 K, at a platinum working electrode, at a scan rate of 50 mV s^{-1}, using SCE as the reference electrode.

Table 4. Electrochemical Data[b] for Complexes 1–5 (Measured in CH_3CN Solution), Other CuNIR Model Complexes with Ligands Containing a Negative Charge, and a Few Native CuNIRs[a]

	Reductive Response		Oxidative Response	
complex	E_{pc}, V	$E_{1/2}$[b], V (ΔE_p[c], mV), E_s[d]	E_{pa}, V	ref
1	−0.35	−0.58 (195), −0.27	+1.27	this work
2	−0.41	−0.51 (110), −0.33 −0.62 (80), −0.28	+1.38	this work
3	+0.03, −0.33 V[e]	−0.50 (130), −0.33	+1.40	this work
4	−0.30	−0.59 (110), −0.32	+1.28	this work
5	−0.53	−0.56 (247), −0.22	+1.30	this work
6	−0.38 (−0.95)[f]	−0.62 (90), −0.32		this work
HL1			+1.45	this work
NaL1 + Zn^{2+}			+1.34	this work
$[Cu^I(HB(3,5\text{-}Me_2Pz)_3)(NO_2)]^-$	+0.08[g]			5g
$[(Ttz^{tBu,Me})Cu^{II}(NO_2)]$	−1.15[h]			5j
Al. Xylosoxidans	+0.240[i]			22a
Ac. Cycloclastes IAM 1013	+0.250[i]			22c
Ps. Chlororaphis DSM 50135	+0.172[i]			22d

[a]Potentials are vs SCE (Fc/Fc^+ couple in CH_3CN, $E_{1/2}$ = +0.43 V), scan rate 50 mV/s, supporting electrolyte: $n\text{-}Bu_4NClO_4$ (0.1 M). [b]$E_{1/2} = (E_{pc} + E_{pa})/2$. [c]$\Delta E_p = E_{pa} - E_{pc}$. [d]$E_s$ is the stripping potential of the oxidation reaction $Cu^0 \rightarrow Cu^{2+}$. [e]Broad shoulder. [f]$E_{1/2}$ for $Co(Cp)_2^{+/0}$ couple (E_{pa} = −0.91 V, E_{pc} = −0.99 V, ΔE_p = 80 mV). [g]E_{pa} vs Fc/Fc^+, measured in CH_2Cl_2. [h]E_{pc} vs SCE, measured in CH_2Cl_2. [i]E vs NHE.

dx.doi.org/10.1021/ic401295t | Inorg. Chem. 2013, 52, 11084–11095

at $E_{1/2}$ = −0.58 V (E_{pc} = −0.67 V, E_{pa} = −0.48 V, ΔE_p = 190 mV) correspond to the $Cu^{II} \rightarrow Cu^{I}$ and $Cu^{I} \rightarrow Cu^{0}$ transformation, respectively. E_{pa} at −0.48 V represents the transformation of the generated Cu^0 species to Cu^I, which is only partial (i_{pc}/i_{pa} ratio ≠ 1). Full transformation of $Cu^0 \rightarrow Cu^{II}$ takes place at the anodic stripping potential of −0.27 V. This response is only observed when the scan has been performed up to −1.2 V that generates Cu^0 species in the vicinity of the working electrode surface. If the scan from 0.0 V up to −0.5 V is performed, then no Cu^0 is formed and, hence, no $2e^-$ reoxidation of $Cu^0 \rightarrow Cu^{II}$ is possible; therefore, this stripping potential at −0.27 V is absent (black trace in Figure 8). One irreversible oxidative response at +1.27 V found for **1** is due to the ligand centered oxidation and not for the $Cu^{II} \rightarrow Cu^{III}$ conversion, as similar irreversible oxidation at +1.34 V has been observed from the CV scan of an equimolar solution of $ZnCl_2$ and NaL1 (see the Supporting Information) in CH_3CN (free HL1 response is at +1.45 V, Supporting Information). Similar redox behaviors of the complexes **3**, **4**, and **5** (see the Supporting Information) have been observed in CH_3CN (see Table 4).

Complex **2**, with a Cu^{II} bound nitrite anion displays three irreversible reductive responses at E_{pc} values of −0.41, −0.57, and −0.66 V, as shown in Figure 9. Among these, the reduction

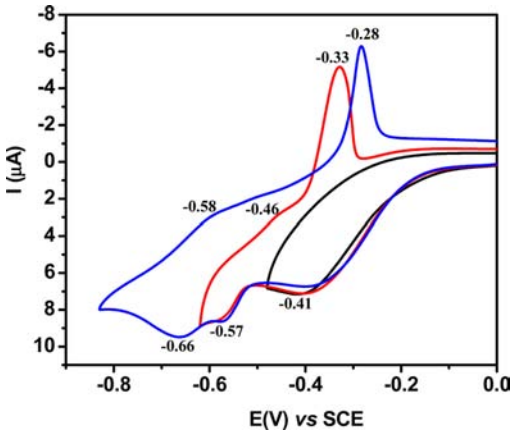

Figure 9. Cyclic voltammograms of **2** in CH_3CN containing 0.1 M $[(n\text{-}Bu)_4N]ClO_4$ as a supporting electrolyte at 298 K, at a platinum working electrode, at a scan rate of 50 mV s^{-1}, using SCE as the reference electrode.

at −0.41 V is due to the $[(L1)Cu^{II}(NO_2)] \rightarrow [(L1)\text{-}Cu^{I}(NO_2)]^-$ transformation; the reverse scan from −0.5 V toward 0.0 V does not show any response that corresponds to the stripping potential(s) at −0.28 V or −0.33 V, observed when the scans have been performed beyond the second or third reduction waves at E_{pc} = −0.57 V and −0.66 V, respectively. Therefore, these two reductions at higher potentials are due to the $Cu^I \rightarrow Cu^0$ transformations of two different Cu^I species generated in situ in the solution (most possibly, one is κ^1-O bound $[(L1)Cu^{I}(ONO)]^-$ and the other is κ^1-N bound $[(L1)Cu^{I}(NO_2)]^-$).

To flip the NO_2 binding mode from κ^1-O → κ^1-N requires time; hence, the cyclic voltammetry measurement with high scan rate should not show the reduction wave that corresponds to the $Cu^I \rightarrow Cu^0$ transformation responsible for the κ^1-N bound Cu^I–NO_2 species. To prove this, variable-scan-rate cyclic voltammetry (CV) measurements of a CH_3CN solution of **2** were performed, as shown in Figure 10. With a scan rate

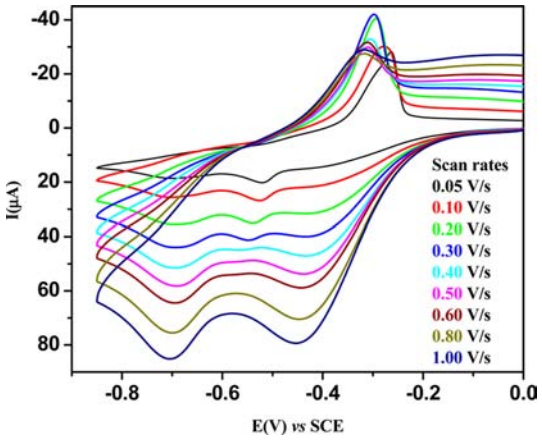

Figure 10. Cyclic voltammograms of **2** in CH_3CN containing 0.1 M $[(n\text{-}Bu)_4N]ClO_4$ as a supporting electrolyte at 298 K, at a platinum working electrode, at various scan rates (given in the legend inset), using SCE as the reference electrode.

up to 400 mV/s or lower, the formation of both Cu^I species was observed, while, above that, the reduction wave that corresponds to E_{pc} at −0.57 V, responsible for $Cu^I \rightarrow Cu^0$ reduction of $[(L1)Cu(NO_2)]^-$ species with κ^1-N bound NO_2^-, has vanished. The potential values clearly reveal that the donor strength of the κ^1-N bound NO_2^- group (E_{pc} = −0.57 V) is less than that of the κ^1-O bound NO_2^- group (E_{pc} = −0.66 V), which is expected, since the negative charge is delocalized to the three atoms of the NO_2^- group, unlike the κ^1-O bound NO_2^- group, where the charge is more localized on one of the O atoms of the bound NO_2^- group. Tanaka and co-workers[4c] reported the redox behavior of $[Cu(H_2O)(tpa)]^{2+}$ (where tpa is *tris*[(2-pyridyl)methyl]amine) in CH_3CN, which shows a reversible Cu^{II}/Cu^I response at $E_{1/2}$ = +0.07 V vs Ag/AgCl (vs SCE, it is +0.025 V), which is comparable to the E_{pc} value of +0.03 V observed for **3** in CH_3CN. Interestingly, they have also reported the electrochemical evidence of formation of two Cu^{II} species such as $[Cu(ONO)(tpa)]^+$ and $[Cu(NO_2)(tpa)]^+$ at −25 °C that display the anodic responses at E_{pa} = −0.20 V and −0.03 V (vs Ag/AgCl) responsible for the $[Cu(ONO)(tpa)]^{+/0}$ and $[Cu(NO_2)(tpa)]^{+/0}$ couples, where κ^1-O and κ^1-N bonded NO_2^- are present, respectively. With neutral tridentate ligands, the reported Cu^I–NO_2 model complexes feature an irreversible oxidative response at $E_{1/2}$ ranging from +0.10 V − +0.27 V vs SCE ($Cu^I \rightarrow Cu^{II}$) which is more anodic than the model complexes containing ligands with a negative charge that may occur at very high negative potential e.g. at −1.15 V vs SCE ($Cu^{II} \rightarrow Cu^{I}$),[5j] as mentioned in Table 4. Complex **6** displays the $Co(Cp)_2^{+/0}$ response at $E_{1/2}$ = −0.95 V (E_{pa} = −0.91 V, E_{pc} = −0.99 V, ΔE_p = 80 mV) and the other two responses, at E_{pc} = −0.66 V and −0.32 V, similar to **2** (see the Supporting Information), as expected. Note that the reported redox potential for the Cu^{II}/Cu^I couple of the type 2 Cu center in CuNIR of *A. Xylosoxidans* measured from pulse radiolysis studies found is at 240 mV[22a] or 230 mV[22b] vs NHE (−0.014 mV or −0.004 mV vs SCE). This potential reported is at 250 mV for *Ac. Cycloclastes* IAM 1013,[22c] at 280 mV for *Al. Xylosoxidans* GIFU 1051[22c] and at 172 mV for *Ps. Chlororaphis* DSM 50135.[22d] The more cathodic Cu^{II}/Cu^I potential of **2** than CuNIR is due to the amidato N^- coordination of $L1^-$ to Cu^{II}, whereas in CuNIR, neutral N_{His} are coordinated to the nitrite bound Cu^{II} ion.

dx.doi.org/10.1021/ic401295t | *Inorg. Chem.* 2013, 52, 11084−11095

According to the mechanisms proposed by Averil, Suzuki, and Hasnain[2a−d] for the catalytic nitrite reduction by CuNIRs, the key reaction intermediate is Cu^{I}−NO_2, which, in the presence of protons, converts $NO_2^- \rightarrow NO(g)$ via an unstable copper nitrosyl. To gain insight to the proton-coupled reduction of nitrite ion, bound to either Cu^{II} or Cu^{I}, we have investigated the reaction of CH_3CO_2H to the Cu^{II} complex **2** and to its coulometrically reduced Cu^{I} form, as well as **6** in CH_3CN. It has been observed that CH_3CO_2H or HCl reacts with **2** in CH_3CN to quantitatively form **5** or **1**, respectively, possibly via simple replacement of the Cu^{II} bound NO_2^- ion and no formation of NO(*g*) has been observed, electrochemically, after the immediate addition of CH_3CO_2H (no redox response within −0.8 V to −1.4 V). The sulfanilamide spectrophotometric method[23] (described in the Supporting Information) supports this notion of NO_2^- liberation.

To check whether the reduced form of **2** in CH_3CN can mimic the nitrite reduction activity functionally, we have coulometrically reduced a solution of **2** (0.96 mmol) at a constant potential of −0.48 V (see the Supporting Information for the UV traces taken during the coulometric reduction), and to this reduced solution was added 2.2 equiv (with respect to **2**) of CH_3CO_2H. During a period of 2−3 min, a cathodic response at −0.93 V was observed, which was obtained due to the reduction of liberated free NO(*g*) in solution; the response increased to a maximum i_{pc} (scans b−e were taken during this time, at a scan rate of 300 mV/s), as shown in Figure 11, that

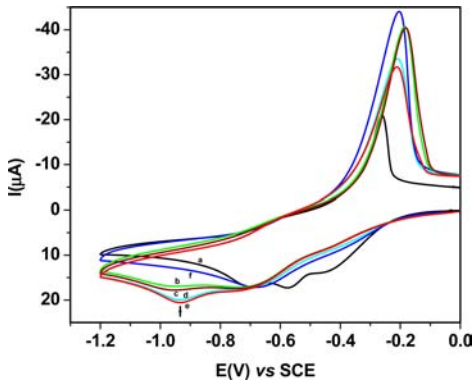

Figure 11. Cyclic voltammograms in CH_3CN containing 0.1 M $[(n\text{-}Bu)_4N]ClO_4$ as a supporting electrolyte at 298 K, at a platinum working electrode at a scan rate of 300 mV s^{-1}, using SCE as a reference electrode: of **2** (0.96 mmol solution, black trace, a), gradual development of 0.93 V response (traces b → e) upon coulometric reduction, followed by CH_3CO_2H reaction, after N_2 purging for 2 min (blue trace, f).

persists for a few minutes; after that, this response started to decrease slowly, because of the loss of NO(*g*) from the solution to the headspace (∼1 mL) of anaerobically closed coulometric cell. After obtaining the maximum i_{pc} value, argon gas was purged for 2 min with stirring and then repeated scans from 0.0 V to −1.2 V do not display the response at −0.93 V, as shown in Figure 11 (blue trace, f) confirming that the reaction product is gaseous (and, most probably, NO(*g*)). If the (L1)Cu(NO) adduct forms, then amidato N^- will be *trans* to the NO, which may accelerate this NO loss.[24] The liberated NO(*g*) has been confirmed from the CV measurement, using the same cell setup and scan rate of a CH_3CN solution of dissolved pure NO(*g*) that displayed the cathodic response at the same potential (see the CV scans of dissolved NO(*g*) of various concentrations, used for plotting the calibration curve (see the Supporting Information)). The identity of this released NO(*g*) has further been confirmed by allowing it to react with a CH_2Cl_2 solution of [Co(TPP)] to generate [Co(TPP)NO],[25] which is characterized via UV-vis (the soret and Q-bands at λ_{max} = 414 and 536 nm, respectively (see the Supporting Information)) and FTIR spectroscopy (after the removal of CH_2Cl_2, the solid obtained displays a value of ν_{NO} = 1693 cm^{-1}; see the Supporting Information). From the calibration curve (I_{max} (μA) vs ppm of NO(*g*), given as Figure S18 in the Supporting Information), the concentration of NO(*g*) liberated has been calculated that is equivalent to the Cu ion concentration. Furthermore, the almost-equal cathodic current peaks at −0.41 V of the CV scan of **2** (black trace), at −0.70 V of the CV scan of the generated **5** (blue trace), and at −0.93 V for that of the in-situ-formed NO(*g*) clearly indicate that an equivalent amount of NO(*g*) and **5** has been formed from the reaction of CH_3CO_2H with the reduced Cu^{I} analogue of **2** in CH_3CN. The isosbestic points of the CV scans shown in Figure 11 at −0.24, −0.60, and −0.69 V reveal a neat transformation of reduced **2** to **5** and NO(*g*), according to the reaction

$$[\mathbf{2}]^- + 2CH_3CO_2H \rightarrow \mathbf{5} + NO(g) + H_2O$$

A similar observation of the CV scans has been observed when $HClO_4$ is used as a proton source (see the Supporting Information). The new cathodic response at −0.83 V is found for the liberated NO gas (NO reduction potential is −0.82 ± 0.2 V, vs NHE);[26] then, the purging argon vanishes and the remaining responses at E_{pc} = −0.57, −0.36, and ∼0.0 V observed (see the Supporting Information) are identical to those found for independently synthesized complex **3** (Supporting Information) in CH_3CN. Therefore, when CH_3CO_2H is used the end product is the acetate bound Cu^{II} complex **5** (Scheme 3, step "i"), whereas when $HClO_4$ is used, then the catalytic cycle is sustained by reforming **3** (see Scheme 3, step "ii"). Similarly, NO(*g*) evolution from the reaction of **6** with CH_3CO_2H has been observed electrochemically (see Figure S22 in the Supporting Information; the observed NO reduction potential is −0.86 V). The reactivity of acids to the CH_3CN solution of either **2** or its reduced form or **6** does not deplete the Cu ion from the ligand, because of the strong σ-donor capability of the monoanionic $L1^-$, and makes amenable this nitrite reductase activity and also stabilizes other complexes with bound H_2O, CH_3OH, and $CH_3CO_2^-$, which are relevant to the catalytic cycle of CuNIR.

■ CONCLUSIONS

$Cu^{II/I}$ complexes relevant to the catalytic cycle of CuNIR have been synthesized and characterized. The principal findings are as follows: the X-ray structure of **2** reveals an asymmetric κ^2-O,O binding mode of NO_2^- to Cu^{II}. In **3**, the Cu^{II} is coordinated by H_2O that is hydrogen-bonded to a solvate H_2O (in CuNIR, the Cu^{II}-coordinated H_2O is hydrogen-bonded to the Asp(98) side chain). This H_2O is replaceable by the NO_2^- ion in CH_3CN solution. Variable-scan-rate cyclic voltammetry (CV) experiments on **2** suggest the flipping of the NO_2^- binding mode from κ^2-O,O to κ^1-N, similar to that observed in CuNIR, according to Averil's mechanism. FTIR supports flipping of the NO_2^- binding mode from κ^2-O,O in **2** → κ^1-N in **6**. Using $Co(Cp)_2$, the Cu^{I} complex **6** was synthesized from precursor **2** (Path-I, Scheme 1). (L1)Cu^{I}−NO_2 formation from the reaction of NO_2^- with (L1)Cu^{I} has also been shown (Path-II, Scheme 1). A coulometrically reduced sample of **2** and

dx.doi.org/10.1021/ic401295t | *Inorg. Chem.* 2013, 52, 11084−11095

independently synthesized Cu^{I} complex **6** react efficiently with CH_3CO_2H or $HClO_4$ to form equivalent amounts of **5** or **3**, respectively, and NO(*g*). With a supporting carboxamide ligand, neither the Cu^{II}–NO_2 nor Cu^{I}–NO_2 model complex of CuNIR is reported. The present set of complexes mimic many of the catalytic steps of CuNIR. The electrochemical technique is used to detect and quantify NO(*g*).

■ ASSOCIATED CONTENT

Supporting Information

FTIR, mass, and ^{1}H NMR spectra of [(*n*-Bu_4N)[(L1)-$Cu^{I}(NO_2)(CH_3CN)$] (Figures S1–S3); EPR of Cu^{II} formed from disproportionation reaction (Figure S4) during the synthesis of [(*n*-Bu_4N)[(L1)$Cu^{I}(NO_2)(CH_3CN)$]; FTIR, mass, ^{1}H NMR, and electronic spectra of **6** (Figures S5–S8); cyclic voltammogram (CV) of $ZnCl_2$ + NaL1 mixture and HL1 itself (Figures S9 and S10); CV of **3**, **4**, **5**, **5** in the presence of CH_3CO_2H, and **6** (Figures S11–S14); calibration curve and experimental details used to determine [NO_2^-] via a spectrophotometric sulfanilamide method (Figure S15); UV–vis traces during the coulometric reduction of **2** (Figure S16); CV of NO(*g*) and standardization plot (Figures S17 and S18); electronic absorption spectra of [Co(TPP)] and [Co(TPP)-NO] (Figure S19); FTIR spectra of [Co(TPP)] and [Co-(TPP)NO] (Figure S20); CV of NO(*g*) generation from the reaction of **2** with $HClO_4$ (Figure S21) and from the reaction of CH_3CO_2H with **6** (Figure S22). X-ray crystallographic data of **1**–**5** are available as a CIF file. This material is available free of charge via the Internet at http://pubs.acs.org.

■ AUTHOR INFORMATION

Corresponding Author

*E-mail: apurba.patra.nitdgp@gmail.com.

Notes

The authors declare no competing financial interest.

■ ACKNOWLEDGMENTS

Financial support from the Department of Science and Technology (DST), Govt. of India (SR/S1/IC-35/2007) is gratefully acknowledged. R.C.M. and S.K.C. acknowledge the support of UGC and CSIR, respectively, for fellowship. We sincerely acknowledge the AvH Foundation, Germany, for the equipment donation grant to procure the CHI-1120A spectroelectrochemical analyzer. We thank the Advanced Light Source, Lawrence Berkeley Lab, for use of beamline 11.3.1 for X-ray data collection. The Advanced Light Source is supported by the Director, Office of Science, Office of Basic Energy Sciences, of the U.S. Department of Energy (under Contract No. DE-AC02-05CH11231). Authors are grateful to R. N. Saha, Department of Chemistry, National Institute of Technology, Durgapur, India, for his help with the spectrophotometric analysis of [NO_2^-].

■ DEDICATION

Dedicated to Prof. R. Mukherjee, IIT Kanpur, on the occasion of his 60th birthday.

■ REFERENCES

(1) (a) Wasser, I. M.; de Vries, S.; Moenne-Loccoz, P.; Schroder, I.; Karlin, K. D. *Chem. Rev.* **2002**, *102*, 1201–1234. (b) Zumft, W. G. *Microbiol. Mol. Biol. Rev.* **1997**, *61*, 533–616.

(2) (a) Averil, B. A. *Chem. Rev.* **1996**, *96*, 2951. (b) Jackson, M. A.; Tiedje, J. M.; Averil, B. A. *FEBS Lett.* **1991**, *291*, 41–44. (c) Kataoka, K.; Furusawa, H.; Takagi, K.; Yamaguchi, K.; Suzuki, S. *J. Biochem.* **2000**, *127*, 345. (d) Antonyuk, S. V.; Strange, R. W.; Sawers, G.; Eady, R. R.; Hasnain, S. S. *Proc. Natl. Acad. Sci. U.S.A.* **2005**, *102*, 12041. (e) Tocheva, E. I.; Rosell, F. I.; Mauk, A. J.; Murphy, M. E. *Science* **2004**, *304*, 867. (f) Leferink, N. G. H.; Han, C.; Antonyuk, S. V.; Heyes, D. J.; Rigby, S. E. J.; Hough, M. A.; Eady, R. R.; Scrutton, N. S.; Hasnain, S. S. *Biochemistry* **2011**, *50*, 4121–4131.

(3) (a) Jiang, F.; Conry, R. R.; Bubacco, L.; Tyeklar, Z.; Jacobson, R. R.; Karlin, K. D.; Peisach, J. *J. Am. Chem. Soc.* **1993**, *115*, 2093–2102. (b) Ruggiero, C. E.; Carrier, S. M.; Tolman, W. B. *Angew. Chem., Int. Ed.* **1994**, *33*, 895–897. (c) Tolman, W. B. *Inorg. Chem.* **1991**, *30*, 4877–4880. (d) Lehnert, N.; Cornelissen, U.; Neese, F.; Ono, T.; Noguchi, Y.; Okamoto, K.; Fujisawa, K. *Inorg. Chem.* **2007**, *46*, 3916–3933. (e) Casella, L.; Carugo, O.; Gullotti, M.; Doldi, S.; Frassoni, M. *Inorg. Chem.* **1996**, *35*, 1101–1113. (f) Beretta, M.; Bouwman, E.; Casella, L.; Douziech, B.; Driessen, W. L.; Gutierrez-Soto, L.; Monzani, E.; Reedijk, J. *Inorg. Chim. Acta* **2000**, *310*, 41–50. (g) Monzani, E.; Anthony, G. J.; Koolhaas, A.; Spandre, A.; Leggieri, E.; Casella, L.; Gullotti, M.; Nardin, G.; Randaccio, L.; Fontani, M.; Zanello, P.; Reedijk, J. *J. Biol. Inorg. Chem.* **2000**, *5*, 251–261.

(4) (a) Schneider, J. L.; Carrier, S. M.; Ruggiero, C. E.; Young, V. G., Jr.; Tolman, W. B. *J. Am. Chem. Soc.* **1998**, *120*, 11408–11418. (b) Komeda, N.; Nagao, H.; Adachi, G. Y.; Suzuki, M.; Uehara, A.; Tanaka, K. *Chem. Lett.* **1993**, 1521–1524. (c) Komeda, N.; Nagao, H.; Kushi, Y.; Adachi, G.; Suzuki, M.; Uehara, A.; Tanaka, K. *Bull. Chem. Soc. Jpn.* **1995**, *68*, 581–589. (c) Arnold, P. J.; Davies, S. C.; Durrant, M. C.; Griffiths, D. V.; Hughes, D. L.; Sharpe, P. C. *Inorg. Chim. Acta* **2003**, *348*, 143–149. (d) Scarpellini, M.; Neves, A.; Castellano, E. E.; Neves, E. F. D.; Franco, D. W. *Polyhedron* **2004**, *23*, 511–518. (e) Woollard-Shore, J. G.; Holland, J. P.; Jones, M. W.; Dilworth, J. R. *Dalton Trans.* **2010**, *39*, 1576–1585. (f) Sarkar, B.; Konar, S.; Gomez-Garcia, C. J.; Ghosh, A. *Inorg. Chem.* **2008**, *47*, 11611–11619. (g) Maiti, D.; Lee, D. H.; Sarjeant, A. A. N.; Pau, M. Y. M.; Solomon, E. I.; Gaoutchenova, K.; Sundermeyer, J.; Karlin, K. D. *J. Am. Chem. Soc.* **2008**, *130*, 6700–6701. (h) Lott, A. L. *J. Am. Chem. Soc.* **1971**, *93*, 5313–5314. (i) Ozarowski, A.; Allmann, R.; Pouribrahim, A.; Reinen, R. *Z. Anorg. Allg. Chem.* **1991**, *592*, 187–201.

(5) (a) Chen, C. S.; Yeh, W. Y. *Chem. Commun.* **2010**, *46*, 3098–3100. (b) Halfen, J. A.; Mahapatra, S.; Wilkinson, E. C.; Gengenbach, A. J.; Young, V. G.; Que, L.; Tolman, W. B. *J. Am. Chem. Soc.* **1996**, *118*, 763–776. (c) Halfen, J. A.; Tolman, W. B. *J. Am. Chem. Soc.* **1994**, *116*, 5475–5476. (d) Halfen, J. A.; Mahapatra, S.; Olmstead, M. M.; Tolman, W. B. *J. Am. Chem. Soc.* **1994**, *116*, 2173–2174. (e) Yokoyama, H.; Yamaguchi, K.; Sugimoto, M.; Suzuki, S. *Eur. J. Inorg. Chem.* **2005**, 1435–1441. (f) Chuang, W.-J.; Lin, I.-J.; Chen, H.-Y.; Chang, Y.-L.; Hsu, S. C. N. *Inorg. Chem.* **2010**, *49*, 5377–5384. (g) Hsu, S. C. N.; Chang, Y.-L.; Chuang, W.-J.; Chen, H.-Y.; Lin, I.-J.; Chiang, M. Y.; Kao, C.-L.; Chen, H.-Y. *Inorg. Chem.* **2012**, *51*, 9297. (h) Kujime, M.; Izumi, C.; Tomura, M.; Hada, M.; Fujii, H. *J. Am. Chem. Soc.* **2008**, *130*, 6088–6098. (i) Kujime, M.; Fujii, H. *Angew. Chem., Int. Ed.* **2006**, *45*, 1089–1092. (j) Kumar, M.; Dixon, N. A.; Merkle, A. C.; Zeller, M.; Lehnert, N.; Papish, E. T. *Inorg. Chem.* **2012**, *51*, 7004. (k) Narin, A. K.; Archibald, S. J.; Bhalla, R.; Boxwell, C. J.; Whitwood, A. C.; Walton, P. H. *Dalton Trans.* **2006**, 1790.

(6) Wright, A. M.; Wu, G.; Hayton, T. W. *J. Am. Chem. Soc.* **2010**, *132*, 14336–14337.

(7) (a) Fujisawa, K.; Tateda, A.; Miyashita, Y.; Okamoto, K.; Paulat, F.; Praneeth, V. K. K.; Merkle, A.; Lehnert, N. *J. Am. Chem. Soc.* **2008**, *130*, 1205–1213. (b) Carrier, S. M.; Ruggiero, C. E.; Tolman, W. B. *J. Am. Chem. Soc.* **1992**, *114*, 4407–4408. (c) Ruggiero, C. E.; Carrier, S. M.; Antholine, W. E.; Whittaker, J. W.; Cramer, C. J.; Tolman, W. B. *J. Am. Chem. Soc.* **1993**, *115*, 11285–11298. (d) Paul, P. P.; Karlin, K. D. *J. Am. Chem. Soc.* **1991**, *113*, 6331–6332. (e) Paul, P. P.; Tyeklar, Z.; Farooq, A.; Karlin, K. D.; Liu, S. C.; Zubieta, J. *J. Am. Chem. Soc.* **1990**, *112*, 2430–2432. (f) Park, G. Y.; Deepalatha, S.; Puiu, S. C.; Lee, D. H.; Mondal, B.; Sarjeant, A. A. N.; del Rio, D.; Pau, M. Y. M.; Solomon, E. I.; Karlin, K. D. *J. Biol. Inorg. Chem.* **2009**, *14*, 1301–1311.

(8) (a) Fraser, R. T. M.; Dasent, W. E. *J. Am. Chem. Soc.* **1960**, *82*, 348−351. (b) Fraser, R. T. M. *J. Inorg. Nucl. Chem.* **1961**, *17*, 265−272. (c) Tran, D.; Skelton, B. W.; White, A. H.; Laverman, L. E.; Ford, P. C. *Inorg. Chem.* **1998**, *37*, 2505−2511.
(9) (a) Tsuge, K.; DeRosa, F.; Lim, M. D.; Ford, P. C. *J. Am. Chem. Soc.* **2004**, *126*, 6564−6565. (b) Sarma, M.; Kalita, A.; Kumar, P.; Singh, A.; Mondal, B. *J. Am. Chem. Soc.* **2010**, *132*, 7846−7847. (c) Sarma, M.; Singh, A.; Gupta, G. S.; Das, G.; Mondal, B. *Inorg. Chim. Acta* **2010**, *363*, 63−70. (d) Sarma, M.; Mondal, B. *Inorg. Chem.* **2011**, *50*, 3206−3212.
(10) (a) Franz, K. J.; Singh, N.; Lippard, S. J. *Angew. Chem., Int. Ed.* **2000**, *39*, 2120. (b) Lim, M. H.; Xu, D.; Lippard, S. J. *Nat. Chem. Biol.* **2006**, *2*, 375. (c) Schneider, J. L.; Young, V. G., Jr.; Tolman, W. B. *Inorg. Chem.* **1996**, *35*, 5410−5411. (d) Mondal, B.; Kumar, P.; Ghosh, P.; Kalita, A. *Chem. Commun.* **2011**, *47*, 2964−2966. (e) Kumar, P.; Kalita, A.; Mondal, B. *Dalton Trans.* **2011**, *40*, 8656−8663.
(11) (a) Naware, M.; Rege, A.; Genov, R.; Stanacevic, M.; Cauwenberghs, G.; Thakor, N. *Proc. IEEE Int. Symp. Circuits Syst.* **2004**, *4*, 25. (b) Hurst, R. D.; Clark, J. B. *Sensors* **2003**, *3*, 321.
(12) Chatterjee, S. K.; Roy, S.; Barman, S. K.; Maji, R. C.; Olmstead, M. M.; Patra, A. K. *Inorg. Chem.* **2012**, *51*, 7625−7635.
(13) *Apex 2, v2.1-0*; Bruker AXS: Madison, WI, 2006.
(14) (a) Sheldrick, G. M. *Acta Crystallogr., Sect. A: Found. Crystallogr.* **1990**, *46*, 467.
(15) Farrugia, L. J. *J. Appl. Crystallogr.* **1999**, *32*, 837.
(16) Sheldrick, G. M. *XP*; University of Göttingen: Göttingen, Germany, 1997.
(17) Nakamoto, K. *Infrared and Raman Spectra of Inorganic and Coordination Compounds, Part B*, Sixth Edition; John Wiley & Sons: Hoboken, NJ, 2009; pp 52−57.
(18) (a) Dyer, J. R. *Applications of Absorption Spectroscopy of Organic Compounds*, Indian reprint M-97, New Delhi-110001; PHI Learning Private, Ltd.: New Delhi, India, 2012; 82 pp. (ISBN 978-81-203-0252-5) (b) Jia, G.; Meek, D. W.; Gallucci, J. C. *Organometallics* **1990**, *9*, 2549.
(19) Geary, W. J. *Coord. Chem. Rev.* **1971**, *7*, 81.
(20) (a) Roy, S.; Mitra, P.; Patra, A. K. *Inorg. Chim. Acta* **2011**, *370*, 247. (b) Roy, S.; Javed, S.; Olmstead, M. M.; Patra, A. K. *Dalton Trans.* **2011**, *40*, 12866.
(21) Merkle, A. C.; Lehnert, N. *Dalton Trans.* **2012**, *41*, 3355−3368 and references therein.
(22) (a) Suzuki, S.; Yamaguchi, K.; Kataoka, K.; Kobayashi, K.; Tagawa, S.; Kohzuma, T.; Shidara, S.; Iwasaki, H.; Deligeer. *J. Biol. Inorg. Chem.* **1997**, *2*, 265. (b) Farver, O.; Eady, R. R.; Abraham, Z. H. L.; Pecht, I. *FEBS Lett.* **1998**, *436*, 239. (c) Kobayashi, K.; Tagawa, S.; Deligeer; Suzuki, S. *J. Biochem.* **1999**, *126*, 408. (d) Pinho, D.; Besson, S.; Brondino, C. D.; de Castro, B.; Moura, I. *Eur. J. Biochem.* **2004**, *271*, 2361.
(23) Clesceri, L. S.; Greenberg, A. E.; Eaton, A. D. *Standard Methods for the Examination of Water and Wastewater*, 20th ed.; American Public Health Association, Washington, DC, 1998; pp 4−112.
(24) (a) Patra, A. K.; Afshar, R.; Olmstead, M. M.; Mascharak, P. K. *Angew. Chem., Int. Ed.* **2002**, *41*, 2512−2515. (b) Patra, A. K.; Rowland, J. M.; Marlin, D. S.; Bill, E.; Olmstead, M. M.; Mascharak, P. K. *Inorg. Chem.* **2003**, *42*, 6812−6823. (c) Afshar, R. K.; Patra, A. K.; Olmstead, M. M.; Mascharak, P. K. *Inorg. Chem.* **2004**, *43*, 5736−5743.
(25) Richter-Addo, G. B.; Hodge, S. J.; Yi, G.; Khan, M. A.; Ma, T.; Caemelbecke, E. V.; Guo, N.; Kadish, K. M. *Inorg. Chem.* **1996**, *35*, 6530.
(26) Bartberger, M. D.; Liu, W.; Ford, E.; Miranda, K. M.; Switzer, C.; Fukuto, J. M.; Farmer, P. J.; Wink, D. A.; Houk, K. N. *Proc. Natl. Acad. Sci. U.S.A.* **2002**, *99*, 10958−10963.